Historical Biology
An International Journal of Paleobiology

ISSN: (Print) (Online) Journal homepage: https://www.tandfonline.com/loi/ghbi20

A new pterosaur specimen from the Lower Cretaceous Yixian Formation of Liaoning Province, China: The oldest fossil record of *Nurhachius*

Masanori Ozeki, David M. Unwin, Phil R. Bell, Daqing Li & Lida Xing

To cite this article: Masanori Ozeki, David M. Unwin, Phil R. Bell, Daqing Li & Lida Xing (26 Jun 2023): A new pterosaur specimen from the Lower Cretaceous Yixian Formation of Liaoning Province, China: The oldest fossil record of *Nurhachius*, Historical Biology, DOI: 10.1080/08912963.2023.2222127

To link to this article: https://doi.org/10.1080/08912963.2023.2222127

HISTORICAL BIOLOGY
https://doi.org/10.1080/08912963.2023.2222127

Taylor & Francis
Taylor & Francis Group

A new pterosaur specimen from the Lower Cretaceous Yixian Formation of Liaoning Province, China: The oldest fossil record of *Nurhachius*

Masanori Ozeki[a,b], David M. Unwin[c], Phil R. Bell[d], Daqing Li[e] and Lida Xing[a]

[a]School of the Earth Sciences and Resources, China University of Geosciences, Beijing, China; [b]Graduate School of Life and Environmental Sciences, University of Tsukuba, Ibaraki, Japan; [c]School of Museum Studies, University of Leicester, University Road, Leicester, UK; [d]Paleoscience Research Centre, University of New England, Armidale, Australia; [e]Institute of Vertebrate Paleontology and Collage of Life Science and Technology, Gansu Agricultural University, Lanzhou, China

ABSTRACT

The Istiodactylidae is one of three ornithocheiroid pterosaur lineages, characterised by a large nasoantorbital fenestrae and labiolingually compressed teeth. Their remains have been reported from Early Cretaceous rocks of northeastern China and Western Europe. A new istiodactylid pterosaur from the upper part of the Yixian Formation (Jingangshan Member) of the Jehol Group, distributed in western Liaoning Province and neighbouring areas, is described on the basis of an incomplete specimen including the partial skull, forelimb and hindlimb bones, and pelvis. This individual, here designated as a referred specimen of *Nurhachius* (*Nurhachius* sp.) is a skeletally almost mature pterosaur with an estimated wingspan of 1.6 m. This specimen is not only the geologically oldest known occurrence of *Nurhachius*, but also a new component of the pterosaur assemblage of the Jingangshan Member, and provides new information on the pelvis and hindlimb of istiodactylids and the palaeobiology of this clade. Considering previous reports of the istiodactylid remains and the geological ages of the strata that yielded them, it is suggested that different istiodactylids existed in Europe and China during the late Barremian.

ARTICLE HISTORY
Received 16 January 2023
Accepted 1 June 2023

KEYWORDS
Istiodactylidae; *Nurhachius*; palaeobiology; Yixian Formation; Pterosauria; Jehol Biota

Introduction

The Jehol Biota from the Yixian and Jiufotang formations in China holds one of the best-preserved terrestrial ecosystems in the Cretaceous worldwide (Xu et al. 2019). The abundance and high quality of fossil preservation makes it an important interval for understanding the origin and early evolution of several major taxonomic groups (e.g. Chang et al. 2008; Xu et al. 2019). Among pterosaurs of the Jehol Biota, istiodactylids comprise at least five genera and six species, including *I. sinensis* Andres and Ji 2006, *Liaoxipterus brachyognathus* Dong and Lü 2005, *Lingyuanopterus camposi* Xu *et al.* 2022, *Luchibang xingzhe* Hone *et al.* 2020, *Nurhachius ignaciobritoi* Wang *et al.* 2005 (= '*Longchengpterus zhaoi* Wang *et al.* 2006'), and *N. luei* Zhou *et al.* 2019. Nearly all of these taxa are exclusive to the Jiufotang Formation, with the exception of *Istiodactylus latidens* (Seeley 1901) (which also occurs in the Wessex and Vectis formations) and *Luch. xingzhe* (which occurs in the Yixian Formation). Despite their apparent diversity, particularly in the Jiufotang Formation, little is known about several aspects of their anatomy, in particular the pelvis and hindlimb (e.g. Wang et al. 2005; Andres and Ji 2006). Here, we describe a new istiodactylid specimen recovered from the Jingangshan Member in the upper part of the Yixian Formation. The new specimen, which includes the skull, partial pelvis and hindlimb, not only adds to the diversity of istiodactylids from this interval but also provides insight into the palaeobiology of this taxon based on the pelvis and sclerotic ring.

Geological setting

The Jehol Group consists of the Yixian, Jiufotang and Fuxin formations, in ascending order (e.g. Pan et al. 2013). The Yixian Formation is a predominantly volcaniclastic unit mainly composed of basalts, andesites and tuffs, with minor tuffaceous sandstone, shale, mudstone, siltstone, and conglomerate (Sha 2007). Sedimentary sequences have been interpreted as representing deposition in a freshwater lake that was affected by the frequent nearby volcanic activity (e.g. Chang et al. 2008). The thickness and lithology of this formation varies for individual sedimentary basins with an estimated maximum thickness of 4,000 m (Jiang and Sha 2006). Four fossil-bearing lacustrine sediments are recognised in the Yixian Formation; the Lujiatun, Jianshangou, Dawangzhangzi, and Jingangshan members, in ascending order (e.g. Chang et al. 2008). Previous radiometric dates obtained from $^{40}Ar/^{39}Ar$ and U-Pb dating indicated that the Yixian and Jiufotang formations span the period ~130 Ma to ~120 Ma (Smith et al. 1995; Swisher et al. 1999; 2002; Wang et al. 2001b, b; He *et al.*, 2004; He et al. 2006). However, the application of more accurate dating methods, such as secondary ion mass spectrometry (SIMS) U-Pb and U-Pb chemical abrasion-isotope dilution-isotope ratio mass spectrometry (CA-ID-IRMS), constrain the duration of the Jehol Group to the period ~126 Ma to ~119 Ma (Yu et al. 2021; Zhong et al. 2021). More specifically, the Jingangshan Member (Undivided Upper Yixian Formation in Zhong et al. 2021) was dated at 125.457 Ma to 124.122 Ma based on CA-ID-IRMS dating of the volcanic tuff layers in the Jianshangou and Huanghuashan units (Zhong et al. 2021).

Materials and methods

The bones of IVPG-P001 are preserved on four slabs, only two of which can be recombined (Figure 1). These fossils were found by

CONTACT Lida Xing xinglida@gmail.com School of the Earth Sciences and resources, China University of Geosciences, No.29, Xueyuan Road, Haidian District, Beijing 100083, China

Supplemental data for this article can be accessed online at https://doi.org/10.1080/08912963.2023.2222127.

Published online 26 Jun 2023

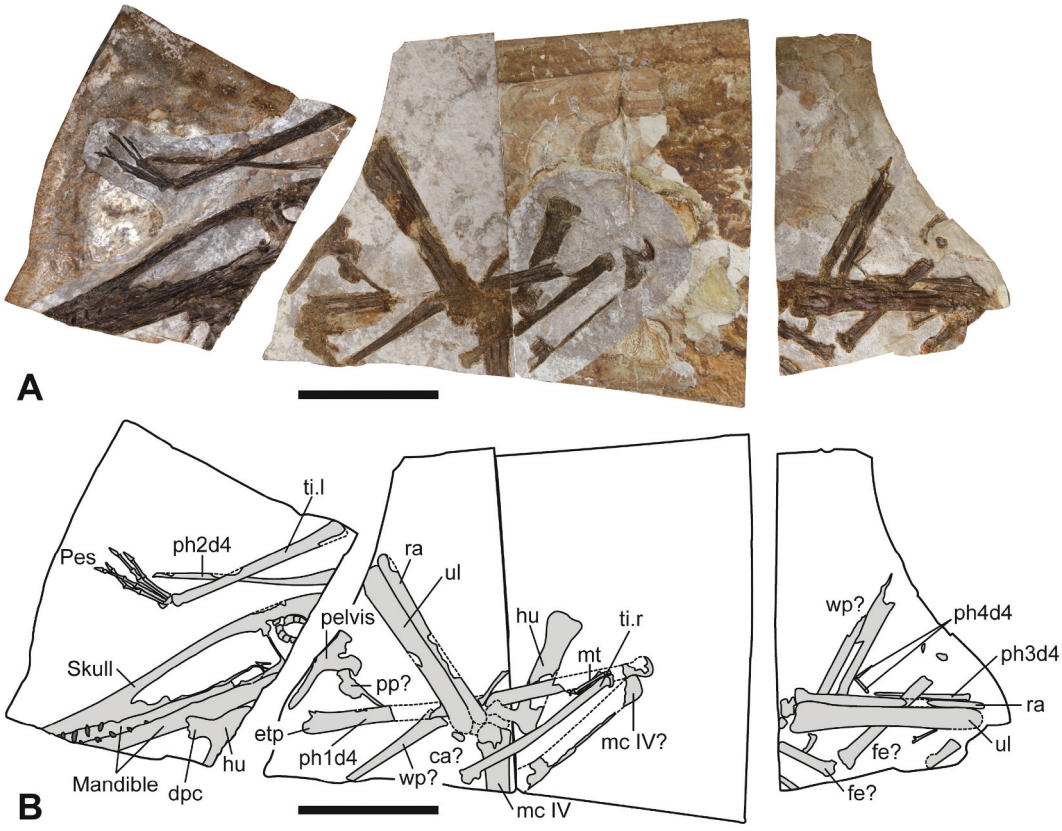

Figure 1. *Nurhachius* sp., referred specimen IVPG-P001. (A) Photograph of the skeleton of IVPG-P001; (B) line drawing of IVPG-P001. **Abbreviations: ca?**, possible carpal; **dpc**, deltopectoral crest of humerus; **etp**, extensor tendon process of the first wing phalanx; **fe?**, possible femur; **hu**, humerus; **mc IV**, metacarpal of digit IV; **mc IV?**, possible metacarpal of digit IV; **mt**, metatarsal; **ph1d4**, manual phalanx 1 of manual digit 4; **ph2d4**, manual phalanx 2 of manual digit 4; **ph3d4**, manual phalanx 3 of manual digit 4; **ph4d4**, manual phalanx 4 of manual digit 4; **pp?**, possible prepubis; **ra**, radius; **ti**, tibia; **ul**, ulna; **wp?**, possible wing phalanx. Scale bar equals 100 mm.

a farmer at a fossil site at Jingangshan in western Liaoning and sent to the Institute of Vertebrate Palaeontology, Gansu Agricultural University. The style of preservation and the colour and composition of these slabs are consistent with rocks found at this locality. There is no duplication among elements and long bone measurements (specifically, ulnae, radii, tibiotarsi) are consistent with having originated from a single individual. Selected measurements of the skull and other elements of IVPG-P001 are shown in Table 1 and 2, respectively.

Measurements of each element and estimation of the wingspan follow the methods of Bennett (2001). This method uses the total length of the humerus, ulna (or radius), metacarpal IV, and the first-to-fourth wing phalanges to estimated the wingspan. The size of the carpus and the width of the body are omitted in order to make the flexion of the articulations between each bone constituting the wing more true to life (Bennett 2001).

To evaluate the phylogenetic position of IVPG-P001, a phylogenetic analysis was performed using TNT (Tree Analysis Using New Technology) ver. 1.5 for Windows (Goloboff and Catalano 2016). This analysis is based on the data matrix of Xu et al. (2022), which was unmodified except for the addition of IVPG-P001. The dataset consists of 81 taxa, and 180 characters or which 41 could be scored for IVPG-P001. The analysis was run via a Traditional Search option with the TBR algorithm and the following settings; Max trees = 100, random seed = 1, 10,000 replicates, and collapsing tree after search (Xu et al. 2022).

Institutional Abbreviations–**BPMC**: Beipiao Pterosaur Museum of China, Liaoning Province, China, **BPV**: Beijing Natural Museum, Beijing, China, **BXGM**: Benxi Geological Museum, Liaoning Province, China, **CAR**: Jilin University, Jilin Province, China, **DLNHM**: Dalian Natural History Museum, Liaoning Province, China, **ELDM**: Erlianhaote Dinosaur Museum, Inner Mongolia, China, **GMN**: Geological Museum of Nanjing, Jiangsu Province, China, **IVPG**: Institute of Vertebrate Palaeontology, Gansu Agricultural University, Gansu Province, China, **IVPP**: the Institute of Vertebrate Palaeontology and Palaeoanthropology, Beijing, China, **JPM**: Jinzhou Museum of Palaeontology, Liaoning Province, China, **NHMUK**: Natural History Museum, London, UK, **NGMC**: National Geological Museum of China, Beijing, China, **PMOL**:

Table 1. Measurements of the cranial and mandibular elements of IVPG-P001. **Symbol: ***, preserved length.

	Measurement (in mm)	
	Length	Width
Skull (premaxilla to parietal)	223*	45.3
Nasoantorbital fenestra	111.6	33.18
Teeth of upper jaw (1, 2, 3, 4)	3.83*, 7.40*, 7.81*, 5.88*	2.44, 3.58, 2.96, 3.07
Dentary (left)	135*	11.17
Teeth of lower jaw(1, 2, 3, 4, 5)	3.01*, 4.09*, 4.14*, 3.81*, 2.82*	2.24, 3.24, 3.11, 3.10, 2.50

Table 2. Measurements of the lengths of the appendicular elements of IVPG-P001. The left and right sides of each bone are indistinguishable in this specimen. **Symbol**: *, preserved length; **, estimated length.

	Measurement (in mm)	
	Length	Width
Humeri	53.42*, 86.96*	15.86
Deltopectoral crest	–	20.71
Ulnae	120*, 140*	14.79, 14.87
Radii	125*, 137*	7.86, 7.07
Metacarpal IV	45*, 107.78*	15.35, 18.96
Wing phalanx I	256**	10.82
Wing phalanx II	131.34*	–
Wing Phalanx III	69.45*	–
Wing phalanx IV	31.18	–
Femurs?	42.74*, 87.90	7.93, 9.79
Tibiae	137.26, 123.28*	8.89, 8.17
Metatarsal I	21.80	–
Metatarsal II	23.32	–
Metatarsal III	24.32	–
Metatarsal IV	18.52	–
Metatarsal V	6.04	–
Metatarsals	20.25, 25.36	–
Pedal digits I (1, 2)	14.64, 9.24	–
Pedal digits II (1, 2, 3)	11.52, 15.81, 9.28	–
Pedal digits III (1, 2, 3)	10.32, 16.68, 7.24	–
Pedal digit IV (1, 2, 3)	13.33, 15.38, 6.82	–

Palaeontological Museum of Liaoning, Shenyang Normal University, Liaoning Provence, China, **XHPM**: Dalian Xinghai Palaeontological Museum, Liaoning Province, China, **ZMNH**: Zhejiang Museum of Natural History, Zhejiang Province, China.

Results

Systematic palaeontology

Pterosauria Kaup, 1834
Pterodactyloidea Plieninger, 1901
Istiodactyliformes Kellner *et al*. 2019
Istiodactylidae Howse, Milner et Martill, 2001 (sensu Andres, Clark, et al., 2014)
Nurhachius Wang *et al*. 2005

Nurhachius sp.

Referred Specimen

IVPG-P001, an incomplete skeleton preserved on four slabs including the incomplete skull and mandible, both humeri, ulnae, radii and metacarpals IV, wing phalanges I–IV, the pelvis and a possible prepubis, a partial femur, both tibiotarsi, and a complete pes.

Locality and Horizon

The Jingangshan Member of the upper Yixian Formation at Jingangshan in western Liaoning, China. Zircons from volcanic tuff layers in the top and middle of the Yixian Formation have provided CA-ID-IRMS ages from 125.457 Ma to 124.122 Ma, indicating a late Early Cretaceous (latest Barremian to earliest Aptian) age for the Jingangshan Member (Zhong et al. 2021).

Description

General comments

The skull and mandible of IVPG-P001 are exposed in left lateral view although a part of the right mandible is also exposed in medial view (Figure 2). They were evidently split along the bedding plane of the slab obscuring most details of the cranial sutures and the surfaces of most elements. The joint between upper and lower jaws cannot be seen because the occipital region posterior to the orbit is missing, as is most of rostrum anterior to the nasoantorbital fenestra. Nevertheless, it is clear that the skull is elongated and relatively low, with a maximum preserved length of 223 mm. The tallest part of the skull is reached above the midpoint of the orbit. The skull preserves two openings: the nasoantorbital fenestra—combining the nasal and antorbital fenestrae—and the anterior part of the orbit. The nasoantorbital fenestra is a subtriangular opening, 111.6 mm in length and 33.18 mm in height. The anterior part of the orbit is damaged, and the outline of this opening remains unclear. Most of the sclerotic ring is preserved within the dorsal part of the orbit and has been deformed into an ellipse. The estimated external and internal diameters of the sclerotic ring are 25.23 mm and 14.95 mm. Regarding the ontogeny of IVPG-P001, the extensor tendon process is fused with the first wing phalanx, and the ischiopubic plate is incompletely fused to the ilium. Therefore, IVPG-P001 is considered to be a subadult individual (OS5~ of Kellner 2015). The smooth external bone surface of some long bones in this specimen supports this designation (Bennett 1993). Almost all forelimb bones are preserved in IVPG-P001, and indicate a wingspan of between 1.6 and 1.7 m. Most istiodactylids have estimated wingspans over 2 m (Table 3), so it is probable that IVPG-P001 would have attained similar dimensions when skeletally mature.

Rostrum

The suture between the premaxilla and maxilla cannot be observed either due to fusion or poor preservation. Nevertheless, the premaxilla presumably forms much of the preorbital part of the skull, including the dorsal border of the nasoantorbital fenestra, where it is a long and narrow bar in shape. This bar becomes slightly curved above the posterior part of the nasoantorbital fenestra. The maxilla, which borders the ventral margin of the rostrum and nasoantorbital fenestra, forms an unusual stepwise anteroventral margin of the nasoantorbital fenestra. The posterior part of the maxilla is obscured by the dentary. The maxilla and premaxilla preserve four teeth in total, although additional teeth were undoubtedly

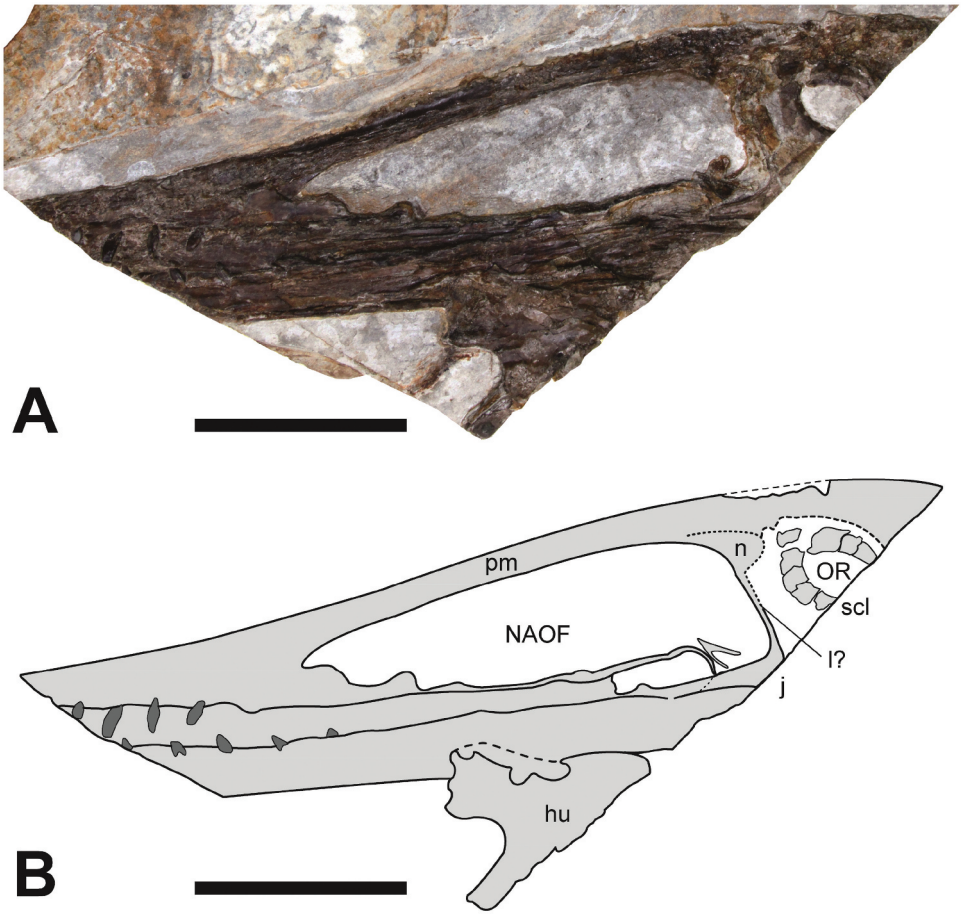

Figure 2. *Nurhachius* sp., referred specimen IVPG-P001. (A) Photograph of the skull and mandible of IVPG-P001; (B) line drawing of the skull and mandible of IVPG-P001. Dashed lines indicate broken part. **Abbreviations: d**, dentary; **f**, frontal; **hu**, humerus; **j**, jugal; **l**, lacrimal; **m**, maxilla; **n**, nasal; **NAOF**, nasoantorbital fenestra; **OR**, orbit; **pa**, parietal; **pf**, prefrontal; **pm**, premaxilla; **scl**, sclerotic ring. Scale bar equals 100 mm.

Table 3. The ratio of the length of each postcranial element to that of the humerus of ELDM 1000 and Chinese istiodactylid pterosaurs. The length of the bones of each taxa was referred to the data or measured based on the photos posted in the following references: IVPP V 13288 (Wang et al. 2005: Fig. 2); NGMC 99–07-011 (Andres and Ji 2006: Table 2); LPM 00023 (Lü et al. 2008: Table 3); ELDM 1000 (Hone et al. 2020: Fig. 1). **Symbol**: *, ratio based on the preserved length of each postcranial element.

		Ratio							
Taxa	Specimen	ul/hu	mc IV/hu	ph1d4/hu	ph2d4/hu	ph3d4/hu	ph4d4/hu	fe/hu	ti/hu
Luchibang xingzhe	ELDM 1000	1.57	1.65	1.99	1.58	1.05	0.50	1.30	1.93
Istiodactylus sinensis	NGMC 99–07-011	1.75	1.25	2.05	1.82	1.46	0.25*	1.04*	1.37
Nurhachius ignaciobritoi	IVPP V 13288	1.74	1.58*	2.00	1.47*	-	-	1.10	1.26
N.ignaciobritoi	LPM 00023	1.77	1.14	2.13	1.78	1.36	-	-	-
Nurhachius sp.	IVPG-P001	1.61*	1.24*	2.94*	1.51*	0.80*	0.36*	0.49*	1.58*

present more anteriorly. There is no indication of a grooved alveolar margin in the upper jaw.

Jugal, Lacrimal and Nasal

The jugal, which in pterosaurs is normally a trifurcate bone, forms the posterior and posteroventral margins of the nasoantorbital fenestra and the anterior and presumably the ventral margins of the orbit. However, because of breakage, only the lacrimal and maxillary processes are preserved. The lacrimal process of the jugal is a delicate bony bar oriented approximately perpendicular to the maxillary process. The more robust maxillary process of the jugal, whose end tapers anteriorly, becomes indistinct anteriorly; however, it seems likely that this process formed up toone-half of the length of the nasoantorbital fenestra. The lacrimal, which is situated between the frontal and the jugal, is a poorly preserved bone that forms the posterior margin of the nasonatorbital fenestra and the anterior margin of the orbit. The nasal appears to have been dislocated slightly from its original anatomical position. It is a semi-elliptical bone and forms the highest apex and posterior margin of the nasoantorbital fenestra, and the anterior margin of the orbit. The suture between the nasal and lacrimal is obscured and other features of this bone cannot be observed.

Prefrontal, Frontal and Parietal

The prefrontal, frontal and parietal are indiscernible from one another, either due to fusion or crushing of the specimen. Together, this unit forms the skull roof and the curved dorsal margin of the orbit, although the precise contribution to these features by each of these elements cannot be determined due to fusion/crushing. No other details in this region can be discerned.

Table 4. The ratio of the length of each postcranial element to that of the humerus and the proportion of each wing phalanges of ELDM 1000 and Chinese tapejarids. The length of the bones of each pterosaurs was referred to the data or measured based on the photos posted in the following references: IVPP V 13363 (Wang and Zhou 2003: Table 2); BPV-077 (Li et al. 2003: Table 1); BPV-078 (Lü and Zhang 2005: Table 1); GMN-03-11-001 (Lü and Yuan 2005: Table 1); D2526 (Jiang and Sha 2006: Table 1); ZMNH M8131 (Lü et al. 2006b: Table 1); D2525 (Lü et al. 2006c: Table 1); BXGM V0011 (Lü et al. 2007: Table 1); GMN-03-11-002 (Lü and Ji 2005: Table 1); IVPP V 14188 (Meng 2008MS: Table 2–2); JPM-2014-005 (Lü et al. 2016: Table 1); XHPM 1009 (Lü et al. 2016: Table 2); IVPP V 23388 (Zhang et al. 2019: Table 3); ELDM 1000 (Hone et al. 2020: Fig. 1).

Specimen	sc/hu	co/hu	ul/hu	ra/hu	mc IV/hu	ph1d4/hu	ph2d4/hu	ph3d4/hu	ph4d4/hu	ph1d4: ph2d4: ph3d4: ph4d4	fe/hu	ti/hu	fi/hu	mt III/ti
'Luchibang xingzhe' (ELDM 1000)	0.64	0.64	1.57	–	1.65	1.99	1.58	1.05	0.50	1.00: 0.79: 0.53: 0.25	1.30	1.83	0.55	0.21
Sinopterus dongi (IVPP V 13363)	0.68	0.61	1.49	1.44	1.61	2.05	1.54	1.11	0.56	1.00: 0.75: 0.54: 0.27	1.25	1.76	0.34	0.20
'Sinopterus gui' (BPV-077)	0.89	0.69	1.49	1.41	–	–	–	–	–	–	0.91	1.85	0.82	–
Eoazhdarcho liaoxiensis (GMN-03-11-002)	0.72	0.61	1.36	1.36	1.50	1.98	1.54	1.03	0.56	1.00: 0.78: 0.52: 0.28	1.04	1.78	–	–
'Eopteranodon lii' (BPV-078)	–	0.51	1.49	1.49	1.58	2.08	1.57	–	–	1.00: 0.76	1.19	–	–	–
'Huaxiapterus jii' (GMN-03-11-001)	–	0.62	1.48	1.46	1.67	2.06	1.61	1.16	0.57	1.00: 0.78: 0.56: 0.28	1.27	1.78	–	0.24
'Eopteranodon' sp. (D2526)	0.67	0.58	1.39	1.36	1.54	1.99	1.49	1.10	0.90	1.00: 0.75: 0.55: 0.45	1.16	1.70	1.04	0.23
'Huaxiapterus' corollatus (ZMNH M8131)	0.73	0.59	1.43	1.38	1.91	2.08	1.36	0.87	0.43	1.00: 0.65: 0.42: 0.20	1.16	1.94	–	0.20
Sinopterus dongi (D2525)	0.51	0.53	1.41	1.40	1.56	1.97	1.43	0.97	0.39	1.00: 0.73: 0.49: 0.20	1.26	1.70	–	0.21
'Huaxiapterus' benxiensis (BXGM V0011)	–	–	1.92	1.92	2.15	2.84	2.24	1.34	–	1.00: 0.79: 0.47	1.81	2.48	–	0.23
Sinopterus lingyuanensis (JPM-2014-005)	–	–	1.19	1.17	1.20	1.57	1.33	0.99	–	1.00: 0.85: 0.63	1.04	1.57	0.56	0.26
'Huaxiapterus' atavismus (XHPM 1009)	–	–	1.41	1.38	1.49	1.90	1.50	1.10	0.70	1.00: 0.79: 0.58: 0.37	0.90	1.61	–	0.27
Sinopterus atavismus (IVPP V 23388)	0.75	0.60	1.45	1.41	1.57	1.97	1.53	–	–	1.00: 0.77	1.25	1.87	0.68	0.23
Sinopterus liui (IVPP V 14188)	0.75	0.63	1.64	1.61	1.66	1.89	–	–	–	–	1.29	1.70	–	0.22

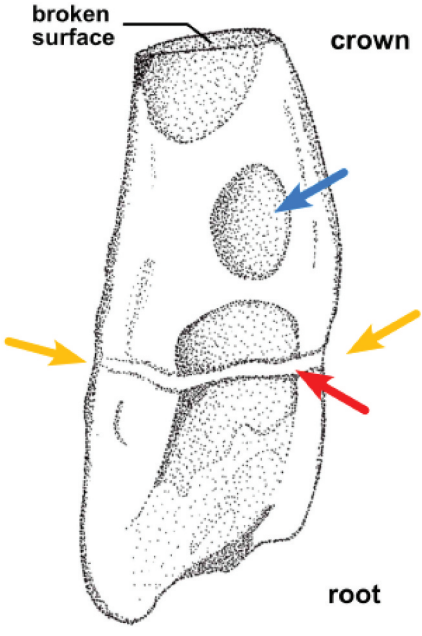

Figure 3. *Nurhachius* sp., upper jaw tooth form of referred specimen IVPG-P001. Blue arrow indicates the concavity on the labial surface. Red arrow identifies the cingulum between crown and root. Yellow arrows indicate the mesiodistal constrictions between crown and root.

Dentary

Only the middle part of the left dentary is preserved. It is a long and shallow bone with parallel dorsal and ventral margins. Its articulation with the post-dentary bones, as well as the shape of the symphysial region, cannot be identified due to breakage at both ends. As preserved, five widely-spaced teeth are present in the anterior half of the jaw. The right dentary, which is missing its posterior part, covers the posterior part of the left maxilla and the anterior part of the jugal.

Dentition

IVPG-P001 preserves nine teeth in total. The four posterior teeth in the upper jaw are all worn or partially broken. The second tooth (as preserved) is the largest although the anterior-most tooth lacks most of the crown and is infilled with calcite. In the maxilla, the posterior-most tooth is situated anterior to the nasoantorbital fenestra. These upper teeth are robust, compressed labiolingually, and elliptical in cross section. The crowns are smooth and lack carinae, and have a slight concavity on the labial surface and a slight constriction between the crowns and roots. The cingulum can be observed between the crown and root (Figure 3). The apex is gently recurved and terminates in a blunt point. Five posterior teeth remain in the alveoli of the lower jaw. In the dentary, the posterior-most tooth is the smallest and occurs posterior to the anterior margin of the nasoantorbital fenestra. The second (as preserved) is the largest tooth in the lower jaw. The widely-spaced mandibular teeth are arranged alternate to the rostral teeth, forming an

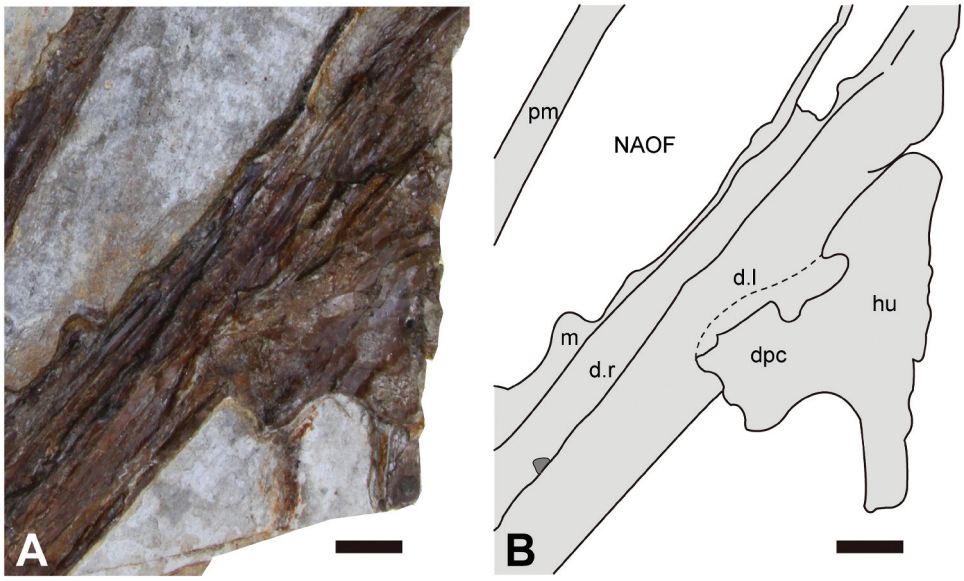

Figure 4. *Nurhachius* sp., the proximal part of the humerus of referred specimen IVPG-P001. (A) Photograph and (B) line drawing of the proximal part of the humerus of IVPG-P001. Dashed lines indicate broken part. **Abbreviations: d**, dentary; **dpc**, deltopectoral crest; **hu**, humerus; **m**, maxilla; **NAOF**, nasoantorbital fenestra; **pm**, premaxilla. Scale bar equals 10 mm.

interlocking dentition when the jaws were closed. The dentary teeth are closely comparable to the maxillary teeth, although the presence of a cingulum cannot be distinguished in the former.

Forelimb bones

The incomplete proximal end of one humerus, including the deltopectoral crest, and the distal half of the other humerus are preserved in two different slabs. It is currently not possible to differentiate left and right elements because of the two-dimensional preservation of the bones. The incomplete proximal humerus is preserved in the same slab as the skull, the deltopectoral crest of which partially covers the dentary (Figure 4). The proximal part of the deltopectoral crest is collapsed, obscuring its proximal margin, but the deltopectoral crest appears anteroventrally deflected. The dorsal margin of this process is proximally convex, suggestive (though not certainly verifiable) of a warped or sinuous margin. The anterior edge of the process is distinctly scalloped, forming a rounded W-shaped margin. The other humerus exhibits an almost straight shaft and a distal end that is only moderately expanded with poorly-defined condyles. Both ulnae and both radii are preserved in articulation with each other. The best preserved ulna is 140 mm in length, with rounded and expanded proximal and distal ends. The best preserved radius is 137 mm in length, with weakly expanded and rounded proximal and distal ends. The shafts of both the ulna and radius are almost straight. The minimum diameter of the radius is about half as wide as that of the ulna. A small subcircular bone located between the ulna and metacarpal IV is possibly one of the carpals, or a sesamoid. All other details of the wrist elements are obscured due to crushing. The proximal part of metacarpal IV is preserved in articulation with the left/right antebrachium. The other metacarpal IV is seemingly represented by an incompletely exposed bone that is preserved on the adjacent slab. The margin of the articulated proximal end is indistinguishable. Four wing phalanges are preserved although no distinction can be made between right and left elements. The first wing phalanx, which is the longest of the preserved appendicular elements, has a slightly curved shaft with expanded proximal and distal ends. A small spur-like projection extending proximally from the proximal end of this wing phalanx is probably the fused extensor tendon process (Figure 1). The second wing phalanx, which is overlain by the tibiotarsus, has a relatively straight shaft with an expanded proximal end and lacks the distal end. The third wing phalanx is straight and gently tapers towards the distal end. The proximal end is obscured. The fourth wing phalanx, which is the shortest of the wing phalanges, is broken into two parts and has a pointed distal end.

Pelvis

The pelvis of IVPG-P001 is exposed in left lateral view (Figure 5). This composite structure is almost complete, except for the loss of the posterior part of the ilium. The pre-acetabular process of the ilium is an elongated anteriorly-projecting process with parallel dorsal and ventral margins that are slightly dorsally concave. The postacetabular process of this specimen is lost, so the relationship between the lengths of anterior and posterior processes of the ilium is unknown. The ischium extends posteriorly, parallel with the pre-acetabular process. The ischium is constricted at its midpoint between the tabular obturator process and the flat distal margin of the ischium. The anterior margin of the pubis is obscured by another bone but was probably relatively straight and not expanded anteriorly, whereas the posterior margin is expanded posteriorly. The angle between the pre-acetabular process and the anterior margin of the pubis is ~125 degrees. These three bones constituting the pelvis are indistinguishably fused to each other and no clear sutures can be discerned; however, the pubis and ischium are not completely fused into the ischiopubic plate. A small concavity between the ilium and ischiopubic plates is probably part of the acetabulum. An incomplete bone covering a part of the pubis may be the prepubis, although details of its morphology are indiscernible.

Hindlimb bones

Both femora are preserved on the same slab but left and right elements cannot be distinguished. The remaining part of the femoral neck is inclined ~70 degrees in relation to the shaft. Both tibiotarsi are preserved, but crushing has obscured details of the proximal and distal ends in both specimens. The left element lies close to the skull and the right tibiotarsus overlies several bones of the forelimb on a separate slab. The former is 137.26 mm long,

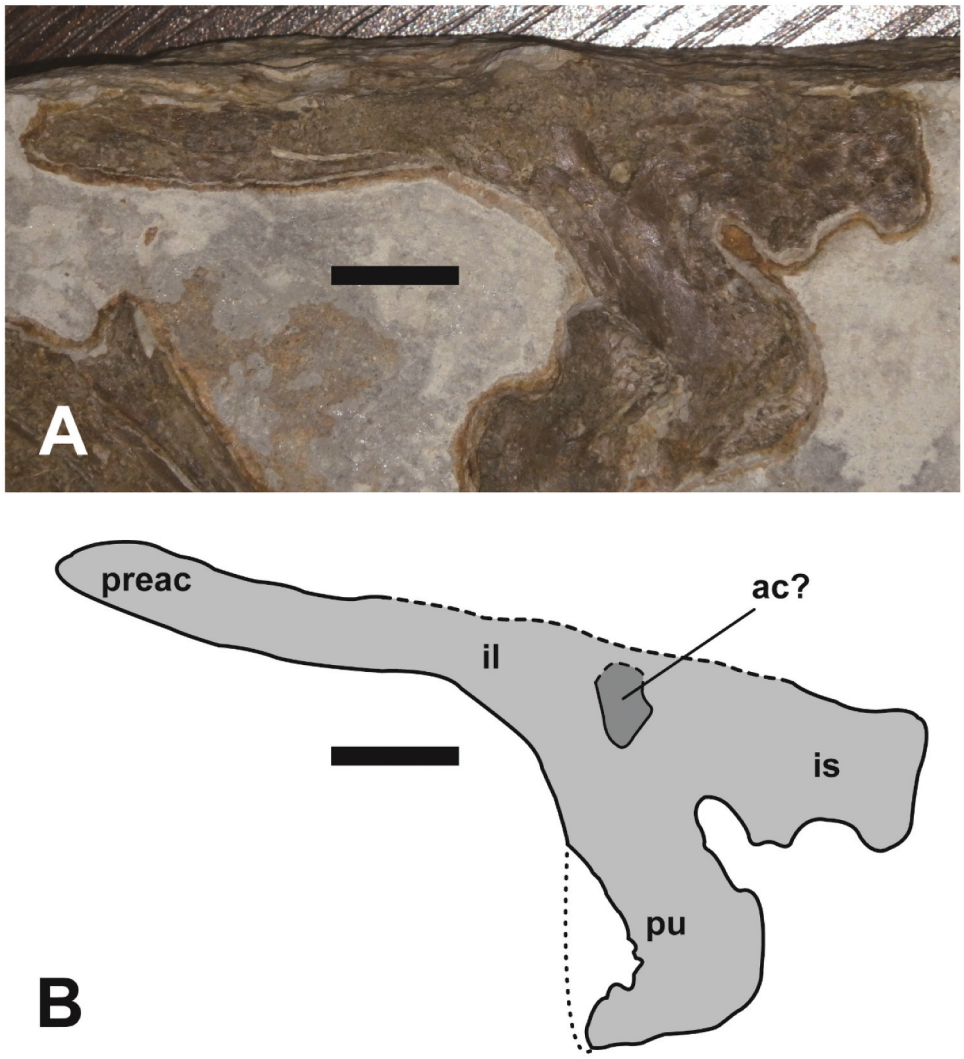

Figure 5. *Nurhachius* sp., pelvis of referred specimen IVPG-P001. (A) Photograph of pelvis of IVPG-P001; (B) line drawing of pelvis of IVPG-P001. Dashed lines indicate broken part, dotted lines indicate reconstructed outline. **Abbreviations: ac?**, possible acetabulum; **il**, ilium; **is**, ischium; **preac**, pre-acetabular process; **pu**, pubis. Scale bar equals 10 mm.

straight and tapers distally. The latter is 123.28 mm long and has a slightly curved shaft. Many bone fragments, which are probably parts of the metatarsals and pedal phalanges, are preserved close to the distal end of the right tibiotarsus. The fibulae are not preserved and may have been highly reduced or lost altogether in this pterosaur. The pes is virtually complete on the left side and appears to exhibit the phalangeal formula 2-3-3-3-0 (Figure 6). However, remains of a suture between the basal phalange and a small discoidal phalange two, now almost fully fused to the distal end of the basal phalange, suggests that digit three consisted of four phalanges, as is typical for pterosaurs. Similarly we suspet that the sall discoidal phalanges two and three of digit four are fused to each other and to the distal end of the basal phalange, though in this case suture lines are not determinable. Consequently, we propose that the true phalangeal formula of the pes was 2-3-4-5-0, as for other pterosaurs. However, fusion of the small intermediate phalanges to preceding phalanges resulted in a pes that is functionally 2-3-3-3-0. Metatarsals I–IV are straight, parallel, subequal in length and have expanded proximal and distal ends. Metatarsal V is a small triangular bone. The pedal phalanges are straight with expanded proximal and distal ends and terminate distally in weakly ginglymous articular surfaces. The terminal unguals are sharply pointed but the curvature of these claws cannot be seen determined.

Remarks

IVPG-P001 can be referred to Pterodactyloidea based on the confluent naris and antorbital fenestra, reduced metatarsal V and loss of pedal digit V (Kellner 2003; Unwin 2003). In addition, this specimen shares with Istiodactyliformes labiolingually-compressed teeth with a cingulum (Kellner et al. 2019), and with Istiodactylidae, labiolingually-compressed teeth that are confined to the anterior of the skull (Xu et al. 2022). IVPG-P001 can be assigned to *Nurhachius* based on the following synapomorphies: triangular, labiolingually-compressed teeth lacking carinae; slight concavity on the labial surface of the tooth; constriction between tooth crowns and roots (Zhou et al. 2019). Two species of *Nurhachius*, comprising a total of three specimens, have been described previously: the holotype and referred specimen of *N. ignaciobritoi* (Wang et al., 2005; Wang et al. 2006), and the holotype of *N. luei* (Zhou *et al*., 2019). The referred specimen of *N. ignaciobrioti* (PMOL-AP00003) was initially described as *'Long. zhaoi'* by Wang et al. (2006), which was subsequently considered a junior synonym of *N. ignaciobritoi* (Lü *et al.* 2008) although there

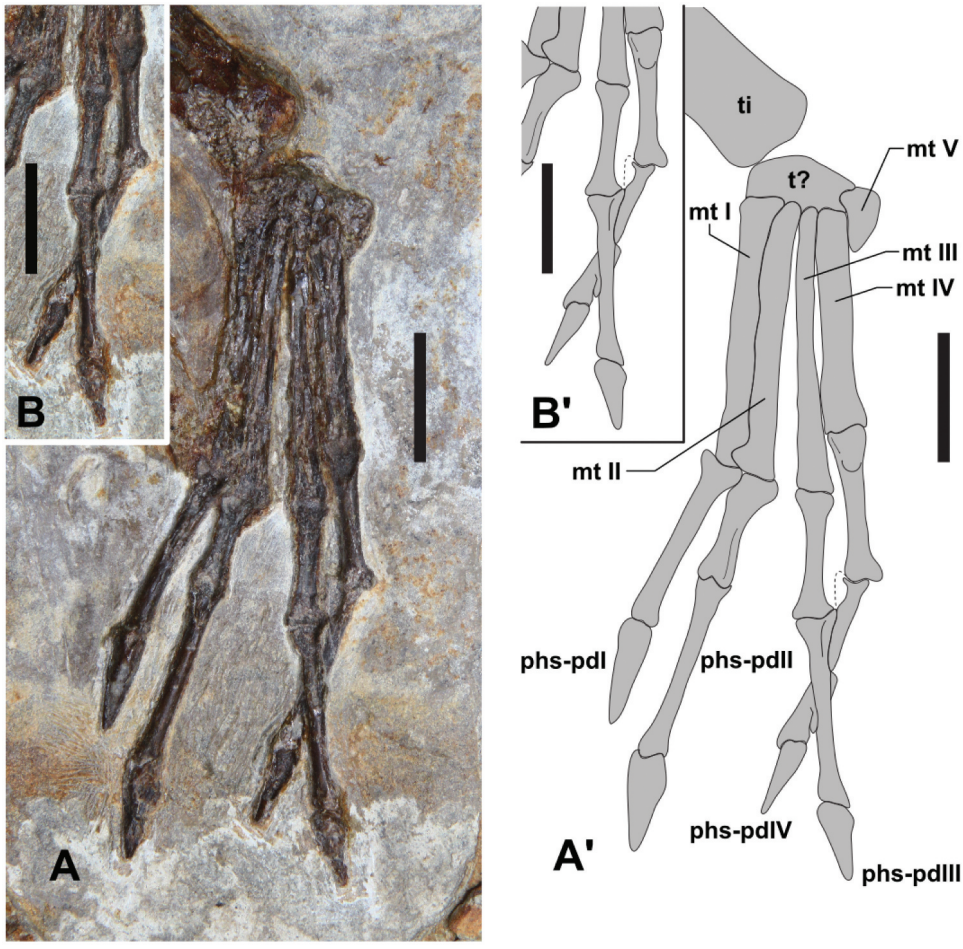

Figure 6. *Nurhachius* sp., pes of referred specimen IVPG-P001. (A)Photograph of pes of IVPG-P001; (B) enlarged photograph of pes digits III and IV of IVPG-P001; (A′) line drawing of pes of IVPG-P001; (B′) line drawing of pes digits III and IV of IVPG-P001. Dashed lines indicate broken part. **Abbreviations: mt I**, metatarsal I; **mt II**, metatarsal II; **mt III**, metatarsal III; **mt IV**, metatarsal IV; **mt V**, metatarsal V; **phs-pdI**, phalanges of pedal digit I; **phs-pdII**, phalanges of pedal digit II; **phs-pdIII**, phalanges of pedal digit III; **phs-pdIV**, phalanges of pedal digit IV; **t?**, possible tarsal(s); **ti**, tibiotarsus. Scale bar equals 10 mm.

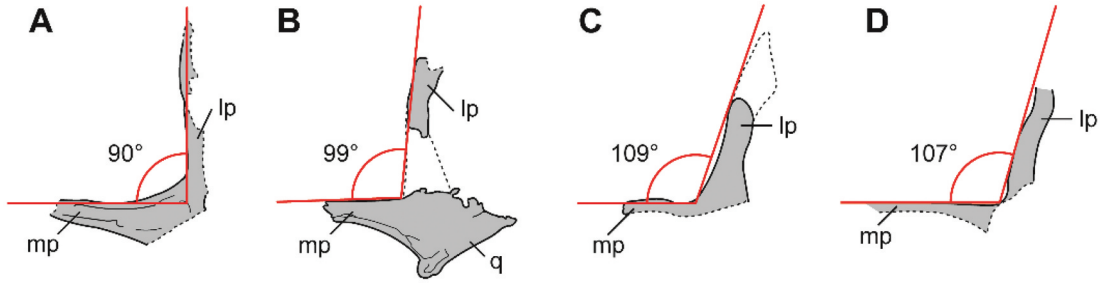

Figure 7. Differences in the inclination of the lacrimal process of the jugal of *Nurhachius* specimens. (A) *Nurhachius* sp., referred specimen IVPG-P001; (B) *N. luei*, holotype BPMC-0204, from Zhou et al. (2019); (C) *N. ignaciobritoi*, holotype IVPP V 13288 from Wang et al. (2005); (D) *N. ignaciobritoi*, referred specimen PMOL-AP00003, from Zhou et al. (2019). **Abbreviations: lp**, lacrimal process; **mp**, maxillary process; **q**, quadrate. No scale.

appears to be no consensus on this latter finding (e.g. Witton 2012, 2013; Kellner et al. 2019). Nevertheless, we follow Zhou et al. (2019) and consider PMOL-AP00003 to be referrable to *N. ignacibritoi*. However, it should be noted that the two specimens of *N. ignaciobritoi* also differ in the proportions of the skull and nasoantorbital fenestra as well as in the relative lengths of some forelimb bones (e.g. the fourth metacarpal and the second wing phalanx of manual digit IV) compared to the length of the humerus.

As for the comparison of IVPG-P001 with other three *Nurhachius* specimens, the poor preservation of this new specimen (e.g. incompleteness of the skull and mandible) makes detailed comparisons with other *Nurhachius* specimens difficult. Consequently, we refer IVPG-P001 to *Nurhachius* sp. in this paper. Since IVPG-P001 was recovered from the Yixian Formation, which is stratigraphically lower than the Jiufotang Formation, this new specimen marks the oldest occurrence of *Nurhachius*. We note, however, that the shape of the jugal in IVPG-P001 differs from that in other *Nurhachius* in that there is a smaller angle between the maxillary and lacrimal processes (Figure 7). This may be taxonomically significant and indicative of a different species

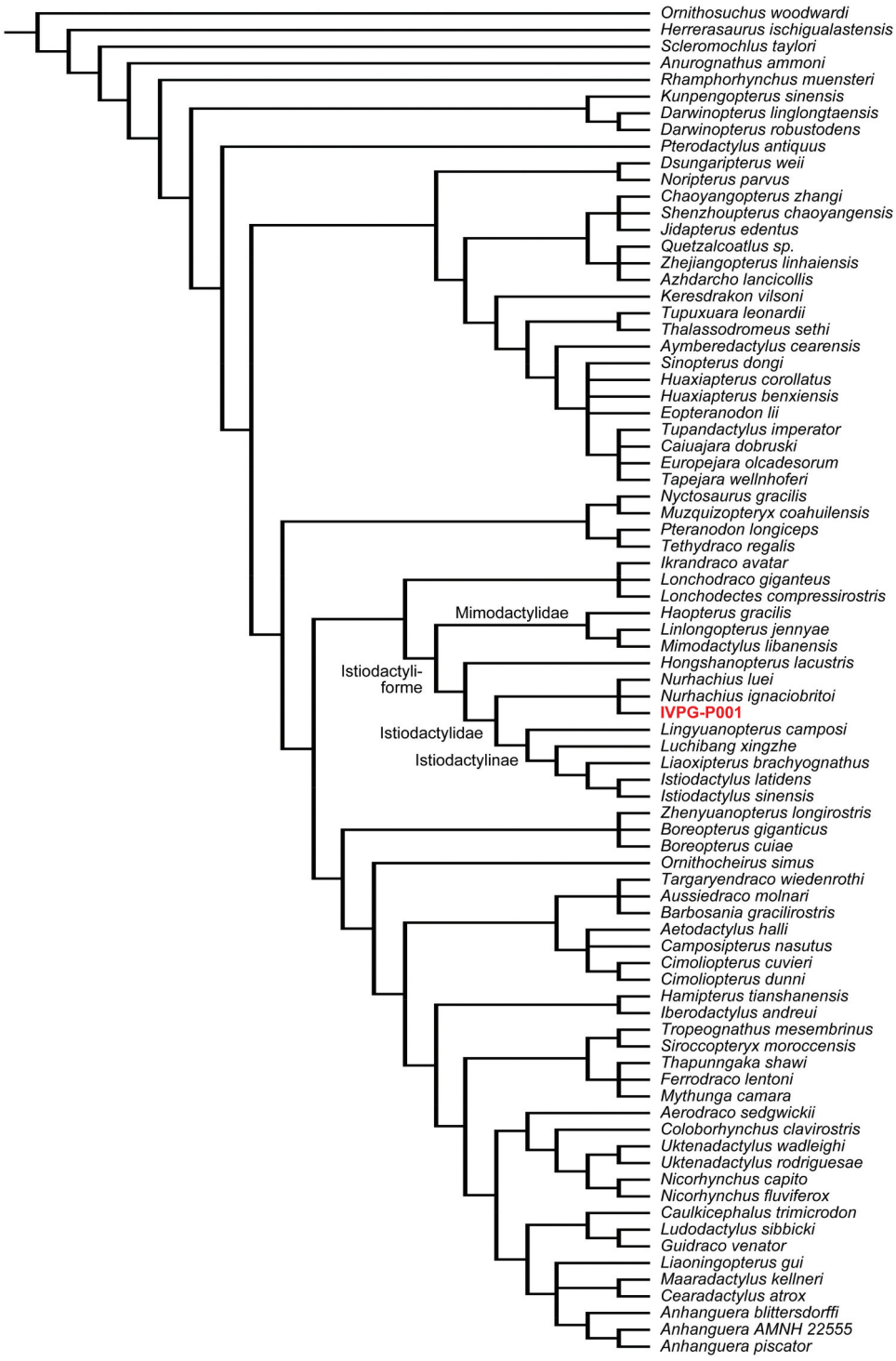

Figure 8. Phylogenetic position of *Nurhachius* sp., referred specimen IVPG-P001. Strict consensus conducted from nine most parsimonious trees.

of *Nurhachius*. In any case, the resolution of the taxonomy of this new specimen awaits more completely preserved specimens of *Nurhachius*.

Phylogenetic analysis

Our phylogenetic analysis resulted in nine most parsimonious trees with a minimum length of 438 steps, and with a consistency index of 0.596 and retaining index of 0.858. In the strict consensus tree, IVPG-P001, *N. luei* and *N. ignaciobritoi* form a polytomy (Figure 8), suggesting that IVPG-P001 falls within the genus *Nurhachius*. This genus is the sister taxa of the subfamily Istiodactylinae, which was defined as the least inclusive clade including *Istiodactylus latidens* (Seeley 1901) but not *Nurhachius ignaciobritoi* Wang *et al.* 2005 by Andres et al. (2014). In our analysis, Istiodactylinae consists of at least four genera (*Istiodactylus, Liaoxipterus, Lingyuanopterus* and *Luchibang*). Within the

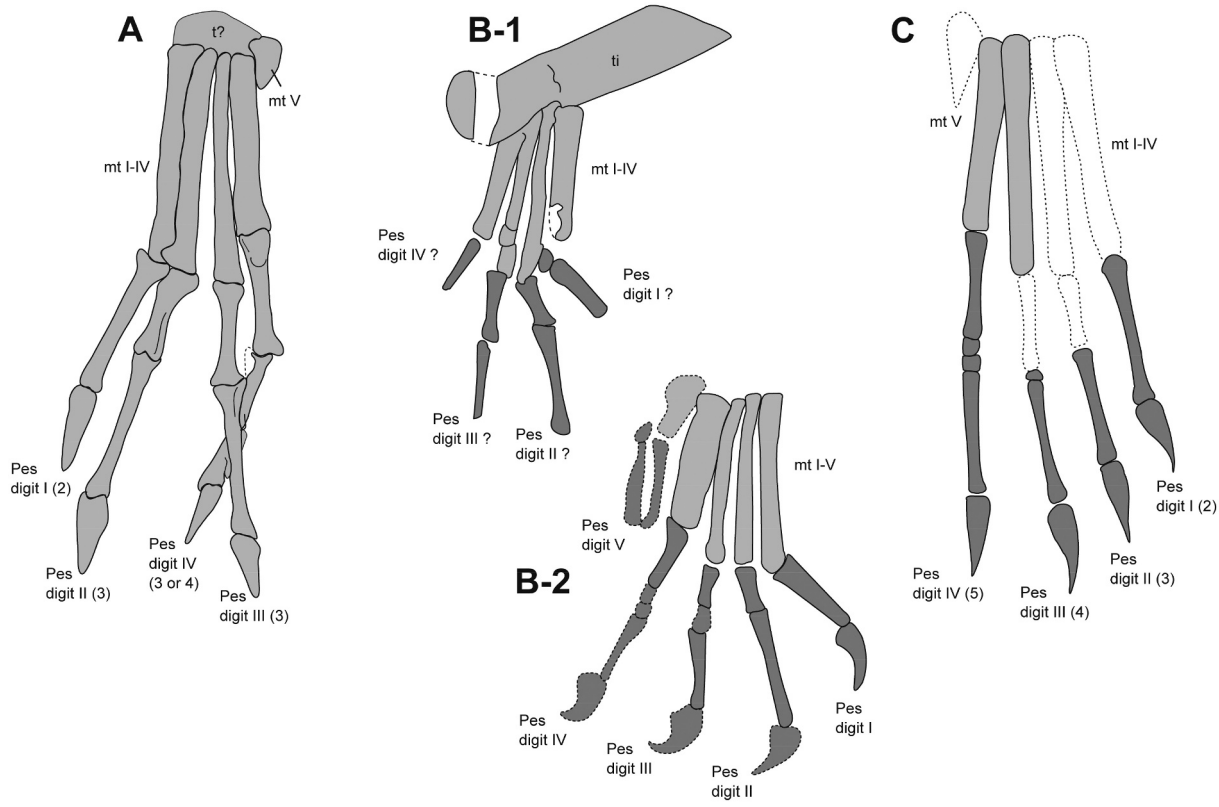

Figure 9. Differences in pedal proportions and morphology of *Nurhachius* specimens. (A) *Nurhachius* sp., referred specimen IVPG-P001; (B-1) *N. ignaciobritoi*, holotype IVPP V 13288; (B-2) *N. ignaciobritoi*, holotype IVPP V 13288 modified from Peters (2011); (C) undescribed specimen of *Nurhachius* from Zhou et al. (2022). Dotted line indicate reconstruct outline and dashed line indicate broken part. **Abbreviations: mt I**, metatarsus I; **mt II**, metatarsus II; **mt III**, metatarsus III; **mt IV**, metatarsus IV; **mt V**, metatarsus V; **t?**, possible tarsal(s); **ti**, tibiotarsus. No scale.

subfamily, *I. latidens* and *I. sinensis* were represented as sister taxa. *Liao. brachyognathus* was recovered as the sister taxon of *Istiodactylus*. *Luch. xingzhe* is the sister taxon of *Istiodactylus* and *Liaoxipterus*. *Ling. camposi* appears as sister taxon to the former three genera (*Istiodactylus* + *Liaoxipterus* + *Luchibang*). These taxa mentioned above form the family Istiodactylidae, and the relationship within this group are harmonious with that shown by Xu et al. (2022). The genus *Nurhachius* is united by the following three synapomorphies in this analysis: orbit shape piriform (char. 6, state 2); teeth crowns with labial and lingual depressions present (char. 126, state 1); and teeth, in labial and lingual view, mesiodistal constriction between crown and root present (char. 127, state 1).

Discussion

Short comment on previously reported specimen ELDM 1000

It is necessary to consider here a recently described 'new istiodactylid' (ELDM 1000) before proceeding to the main discussion. ELDM 1000 was originally reported by Hone and Xu (2018) who suggested that this specimen might be a chimera that combines fossils from two different taxa, specifically an istiodactylid and an azhdarchoid. This specimen was later made the holotype of *Luchibang xingzhe* by Hone et al. (2020) and identified as an istiodactylid. Hone et al. (2020) regarded ELDM 1000 as a single individual (i.e. not a chimera) mainly based on the following three grounds: the ratio of the size of skull to estimated wingspan is consistent with that of other istiodactylids; the relationship between bone and matrix is harmonious with no evidence of tampering, and; there is no trace of large artificial repairs (Hone et al. 2020).

As described in Hone et al. (2020), the skull of ELDM 1000 is verifiably from an istiodactylid pterosaur on the basis of its characteristic tooth shape and arrangement, and the size of its nasoantorbital fenestra. However, the shapes and proportions of postcranials of ELDM 1000 differ from the descriptions of Hone et al. (2020). First, the shape of the deltopectoral crest of ELDM 1000 deviates from that of other ornithocheiroids. This crest in ornithocheiroids is warped (Unwin 2003), and its distal margin curves dorsally. The crest of ELDM 1000 does not show this ornithocheiroid characteristic (Unwin 2003). Instead, the distal margin is parallel to the proximal margin, so the crest of ELDM 1000 is sub-rectangular in shape; a character considered to be a synapomorphy of Lophocratia (Unwin 2003). The coracoid of ELDM 1000 also differs from that of typical ornithocheiroids. This bone expands at the proximal end and bears a well-developed coracoid flange. This flange is present in tapejaroid pterosaurs (Frey et al. 2003) and a similar structure can be observed in Chinese tapejarids (e.g. *Sinopterus*). On the other hand, no istiodactylids reported so far show these characteristics. In ELDM 1000, the ratio of the length of the ulna to that of the humerus is 1.57, which is smaller than other istiodactylids (Table 3). By contrast, the ratio of the length of the fourth wing phalanx to that of the first wing phalanx (= 0.25) is much larger than that of istiodactylids but is similar to that of *Sinopterus* (Table 3, 4). In addition, the ratios of the lengths of the other appendicular elements in ELDM 1000 are remarkably similar to those of the holotype of *Sinopterus dongi* (IVPP V 13363). In light of this similarity in morphology, the postcranial

skeleton of ELDM 1000 is almost certainly not that of an istiodactylid pterosaur but of a specimen of *S. dongi*, or a closely related taxon. Furthermore, the observation that the relationship between the lengths of the humerus and hindlimb (femur + tibiotarsus) of ELDM 1000 match that of an azhdarchoid rather than that of pteranodontoid or ornithocheiroid (Hone et al. 2020) is expected if the postcranium of ELDM 1000 is from a non'istiodactylid pterosaur. Darwinopterans, a group of pterosaurs reflecting the transitional stage from 'basal' to more 'derived' froms (e.g. Lü et al. 2010) might be cited as evidence that ELDM 1000 might not be a chimera because darwinopterans exhibit a mosaic combination of plesiomorphic characters (e.g. elongate metatarsal V and tail) typical of 'rhamphorhynchoid' pterosaurs and more derived characters (e.g. a nasoantorbital fenestra and absence of cervical ribs) typical of pterodactyloids (Lü et al. 2010, Wang et al. 2010). While ELDM 1000 is suggested to exhibit characteristics of at least two different pterosaur clades; (e.g. tooth shape and enlarged nasoantorbital fenestra typical of istiodactylids; proportionally long hindlimb and wing phalanges of azhdarchoids; Hone and Xu 2018), this observation is also consistent with the proposal that ELDM 1000 is a chimera (istiodactylid and azhdarchoid). For these reasons, the taxon name *Luch. xingzhe* is treated here as referring only to the skull and mandible of ELDM 1000.

Palaeobiology of *Nurhachius*

The pelvis of IVPG-P001 is the most complete of any istiodactylid described to date (Witton 2013). Only disarticulated and poorly preserved pelvic elements have been described so far for *I. sinensis* (Andres and Ji 2006) and *N. ignaciobritoi* (Wang *et al.* 2005); however, the nearly complete pelvis of IVPG-P001 is preserved and visible in lateral view. The orientation of the pre-acetabular process and the large angle between the pre-acetabular process and the anterior margin of the pubis, is similar to that of ornithocheiroid pterosaurs (Hyder et al. 2014), indicating that at least some istiodactylids, such as IVPG-P001, held their bodies in a relatively erect stance on the ground. Furthermore, this specimen has unusual characteristics in the pedal digits. The typical pedal phalangeal formula for Pterodactyloidea is 2-3-4-5-1 (or 0) (e.g. Witton 2013) although the third and fourth digits have small intermediate cartilaginous phalanges in young individuals that ossify with increasing maturity (Wellnhofer 1991). The number of phalanges in digits I–V of IVPG-P001 (phalangeal formula 2-3-3-3-0; Figure 9A) is reduced compared to other pterodactyloids but is consistent with the formula given for *N. ignaciobritoi*, as far as it is preserved (Fig. 9B-1). However, Peters (2011) shows a reconstruction of foot of the holotype of *N. ignaciobritoi* with a phalangeal formula of 2-3-4-5-3 (Fig. 9B-2). Zhou et al. (2022) also mentioned an undescribed specimen of *Nurhachius* (PMOL-AP00034), and illustrated it with a pedal formula of 2-3-4-5-0 (Figure 9C). In further comparison to PMOL-AP00034, IVPG-P001 has a relatively shorter metatarsal V and a slightly smaller length ratio between the penultimate and proximal phalanges in the third digit. Regarding the ratio of the length of each pedal digit to that of the metatarsals, overall, the ratios in IVPG-P001 are greater than those of PMOL-AP00034, with a relatively long second pedal digit. The reconstruction of *N. ignaciobritoi* illustrated by Peters (2011) depicts a relatively longer fifth metatarsal than that of IVPG-P001. The relative length of the penultimate phalanx of the third digit of IVPG-P001 is considerably shorter than that of the reconstruction of *N. ignaciobritoi*, but the relative length of the fourth digit is similar in both specimens. It is not clear whether these

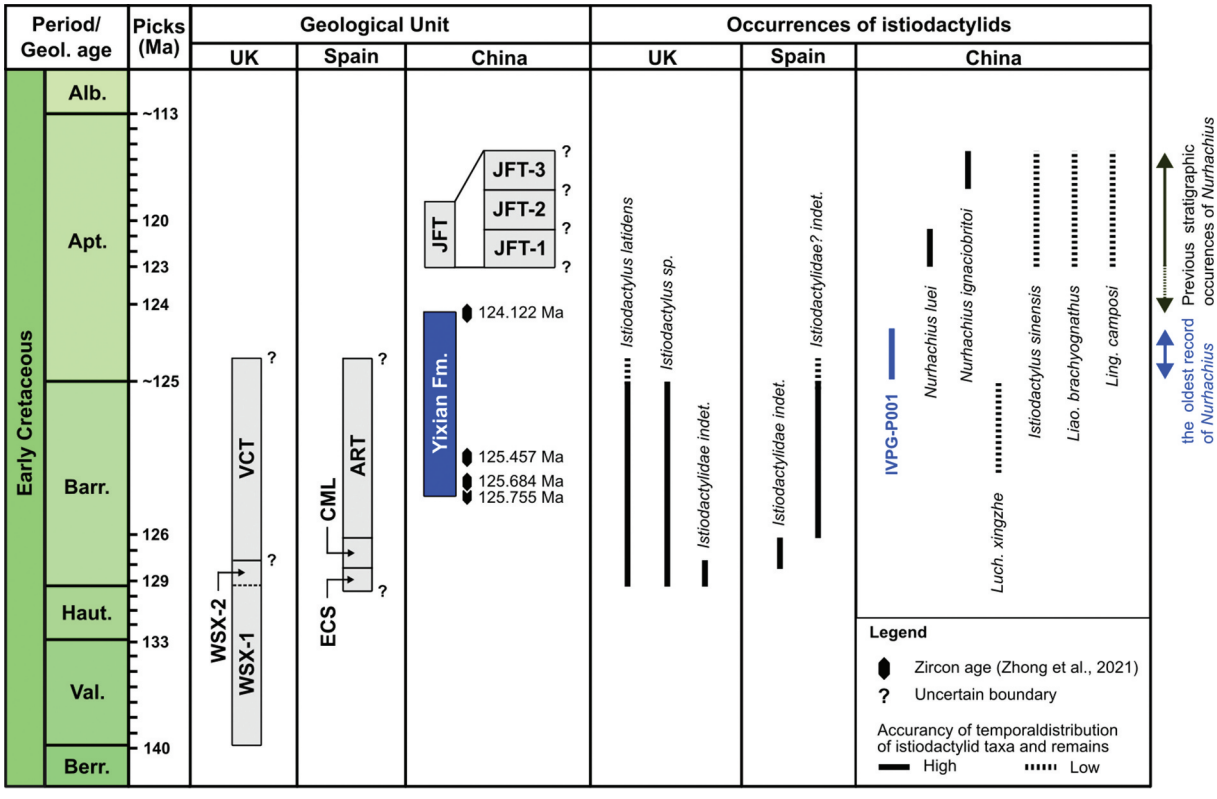

Figure 10. Relationships between the stratigraphic horizons of istiodactylid specimens and their geological ages. Each geological age is based on Martill et al. (2011), Sánchez-Hernández et al. (2007), Zhong et al. (2021) and Yu et al. (2021). **Abbreviations: ART**, Artoles Formation; **CML**, Camarillas Formation; **ECS**, El Castellar Formation; **JFT**, Jiufotang Formation (JFT-X corresponds to Bed-X in Wu et al. 2018); **VCT**, Vectis Formation; **WSX-1**, Wessex Formation unexposed on the Isle of Wight; **WSX-2**, Wessex Formation exposed on the Isle of Wight.

differences reflect autapomorphies, ontogenetic variation, or other factors, and more specimens are needed to resolve these questions.

Schmitz and Motani (2011) examined the diel activity (e.g. nocturnal vs diurnal) of some archosaurs and pointed out that diurnal animals have a sclerotic ring with a relatively small internal diameter compared to the external diameter. Conversely, nocturnal animals have a sclerotic ring with a relatively large internal diameter compared to the external diameter. They suggested the possibility that the relative proportion of these elements is an indicator of daily activity patterns in archosaurs (but see critique of this method by Hall et al. 2011). IVPG-P001 preserves a partial sclerotic ring and the inferred sclerotic ring of this specimen has a small internal diameter (41.3 mm) relative to the external diameter (65.7 mm). This characteristic suggests that IVPG-P001 was potentially diurnal, although we concede that there are possible flaws with this method (Hall et al. 2011). Direct evidence for the diet of istiodactylids is lacking, although they have been variously interpreted as piscivorious (e.g. Hooley 1913), carnivorous (e.g. Witton and Farke 2012, 2013; Martill 2014; Bestwick et al. 2020), insectivorous (Lü et al. 2008; Lü 2015; but see Jiang et al. 2020), or possibly scavengers (e.g. Howse et al. 2001). The teeth of *Nurhachius* differ from those of other istiodactylids in having smooth surfaces, no carinae, and a slight concavity in the crown. *Nurhachius* was possibly a pterosaur foraging during the day.

Temporal and geographic distribution of istiodactylid pterosaurs

Istiodactylid pterosaurs have so far only been recovered from the Lower Cretaceous of Europe (specifically, Spain and England) and China. Reports of this clade from Spain are restricted to isolated teeth from the Camarillas Formation (lower Barremian; 'morphotype 4' of Sánchez-Hernández et al. 2007) and the Artoles Formation (upper Barremian to lower Aptian; Ruiz-Omeñaca et al. 1997). It has also been pointed out that the teeth from these two formations differ in morphology from each other (Sánchez-Hernández et al. 2007). In England, istiodactylids have been reported only from the Barremian to early Aptian Wealden Group on the Isle of Wight. The Wealden group is composed of Wessex and Vectis formations (in ascending order), both of which have produced istiodactylid remains. The Wessex Formation has mainly yielded isolated teeth, which indicate the coexistence of multiple istiodactylid species (Sweetman and Martill 2010; Martill et al. 2011). Several partial skulls and mandibles have been described from the Vectis Formation, which indicate the presence of at least two species (Hooley 1913; Howse et al. 2001; Martill et al. 2011; Witton and Farke 2012; Martill 2014; Averianov et al. 2021). Chinese istiodactylids are by far the most diverse (in terms of named taxa) and have been reported from the Lower Cretaceous Yixian and Jiufotang formations of the Jehol Group. The only istiodactylid from the Yixian Formation is *Luchibang*, and although the original description did not mention the exact horizon of this specimen (Hone et al. 2020), it is considered that it came from either the Jianshangou or the Dawangzhangzi member in the lower and middle part of the Yixian Formation (Jiang et al. 2021). The detailed stratigraphic occurrences of most of the istiodactylids from the Jiufotang Formation (*I. sinensis, Liao. brachyognathus*, and *Ling. camposi*) are unknown, except for three specimens of *Nurhachius* (Dong and Lü, 2005; Andres and Ji 2006; Xu et al. 2022). Based on the subdivision of the Jiufotang Formation proposed by Wu et al. (2018), it is considered that *N. luei* and both specimens of *N. ignaciobritoi* originated from Bed 1 (lower part) and Bed 3 (upper part), respectively (Wu et al. 2018; Zhou et al. 2019). The biostratigraphic relationships of each of these forms (Chinese, Spanish, and English) is shown in Figure 10.

Based on current dating of the Jehol Group, the Jingangshan Member corresponds to the earliest Aptian and may extend to the latest Barremian, whereas the Dawangzhangzi and Jianshangou members, which are stratigraphically lower than the Jingangshan Member, correspond to the late Barremian (Zhong et al. 2021). The Yixian Formation in China, therefore, partially overlaps the Artoles and Vectis formations in Europe which are late Barremian in age. Previous reports show that the oldest-known istiodactylid pterosaurs come from the earliest Barremian, and that multiple istiodactylid taxa already existed in Europe during this interval. The discovery of *Luchibang*, the oldest Chinese istiodactylid, indicates that different istiodactylids coexisted in Europe and China during the late Barremian, and migration from Europe to China may have occurred before this period. Considering reports of istiodactylid remains from different horizons of the Yixian Formation, a certain degree of diversity is apparent and it is possible that unique pterosaur assemblages existed in each formation/region, although little is known of their specific taxonomy. The Aptian record of istiodactylids is almost exclusively restricted to China, where they appear to have flourished. Based on the occurrence of *Luchibang* and *Nurhachius* (IVPG-P001), the radiation of Chinese istiodactylids appears to have been initiated during the deposition of the Yixian Formation. The younger Jiufotang Formation represents the peak diversity of istiodactylids found anywhere in the world. With the discovery of the new *Nurhachius* specimen, the genus *Nurhachius* is recorded for the first time from the Yixian Formation making it the only one of the five genera of istiodactylids currently known from the Jehol Group, to occur in both the Yixian and Jiufotang formations.

Acknowledgments

The authors thank two anonymous reviewers for their helpful comments on the previous version and editor Gareth Dyke for his kind attention to our manuscript.

Disclosure statement

No potential conflict of interest was reported by the author(s).

ORCID

Masanori Ozeki http://orcid.org/0000-0002-6405-3262
Daqing Li http://orcid.org/0000-0001-5952-4747
Lida Xing http://orcid.org/0000-0003-3923-9206

References

Andres B, Clark J-M, Xu X. 2014. The earliest pterodactyloid and the origin of the group. Curr Biol. 24(9):1011–1016. doi:10.1016/j.cub.2014.03.030.
Andres B, Ji Q. 2006. A new species of *Istiodactylus* (Pterosauria, Pterodactyloidea) from the lower cretaceous of liaoning, China. J Vert Paleont. 26(1):70–78. doi:10.1671/0272-4634200626[70:ANSOIP]2.0.CO;2.
Averianov AO, Kolchanov ZNG VV, Aleksandrova GN, Yaroshenko OP, Yaroshenko OP. 2021. The wandering jaws of *Istiodactylus latidens* (Pterosauria, Istiodactylidae). Cretaceous Res. 126:104887. doi:10.1016/J.CRETRES.2021.104887
Bennett SC. 1993. The ontogeny of *Pteranodon* and other pterosaurs. Paleobiology. 19(1):92–106. doi:10.1017/S0094837300012331.
Bennett SC. 2001. The osteology and functional morphology of the late cretaceous pterosaur *Pteranodon* Part I. General description of osteology. Palaeontogr Abt A. 260(1–6):1–112. doi:10.1127/pala/260/2001/1.

Bestwick J, Unwin DM, Butler RJ, Purnell MA. 2020. Dietary diversity and evolution of the earliest flying vertebrates revealed by dental microwear texture analysis. Nat Commun. 11:5293. doi: 10.1038/s41467-020-19022-2.
Chang M-M, Chen P-J, Wang Y-Q, Wang Y, Miao D-S eds. 2008. The Jehol Biota: The Eergence of Feathered Dinosaurs, Beaked Birds and Flowering Plants. Shanghai: Sjanghai Scientific and Technical Publishers and Elsevier; 208 pp.
Dong Z-M, Lü J-C. 2005. A new Ctenochasmatid Pterosaur from the early cretaceous of Liaoning Province. Acta Geol Sin-Engl. 79(2):164–167. doi:10.1111/j.1755-6724.2005.tb00878.x.
Frey E, Buhy MC, Martill DM. 2003. Middle- and bottom-decker cretaceous pterosaurs: unique designs in active flying vertebrates. Vol. 217 London: Geol Soc Spec Publ; p. 267–274. doi:10.1144/GSL.SP.2003.217.01.15.
Goloboff PA, Catalano SA. 2016. TNT version 1.5, including a full implementation of phylogenetic morphometrics. Cladistics. 32(3):221–238. doi:10.1111/cla.12160.
Hall MI, Kirk EC, Kamilar JM, Carrano MT. 2011. Comment on "Nocturnality in dinosaurs inferred from scleral ring and orbit morphology". Science. 334 (6063):1641. doi:10.1126/science.1208442.
He H-Y, Wang X-L, Zhou Z-H, Jin F, Wang F, Yang L-K, Ding X, Boven A, Zhu R-X. 2006. 40 Ar/ 39 Ar dating of Lujiatun Bed (Jehol Group) in Liaoning, northeastern China. Geophys Res Lett. 33(4):L04303. doi:10.1029/2005GL025274.
Hone DWE, Fitch AJ, Ma F-M, Xu X. 2020. An unusual new genus of istiodactylid pterosaur from China based on a near complete specimen. Palaeontol Electron. 23:a09. doi:10.26879/1015
Hone DWE, Xu X, 2018. An unusual and nearly complete young istiodactylid from the Yixian Formation, China. Flugsaurier 2018: the 6th International Symposium on Pterosaurs. Los Angeles, USA, Abstracts: 53–56.
Hooley RW. 1913. On the Skeleton of *Ornithodesmus latidens*; an Ornithosaur from the Wealden Shales of Atherfield (Isle of Wight). Quart J Geol Soc. 69 (1–4):372–421. doi:10.1144/GSL.JGS.1913.069.01-04.23.
Howse SCB, Milner AR, Martil DM. 2001. Pterosaurs. In: Martil DM, Naish D, editors. Dinosaurs of the Isle of Wight Field Guide to Fossils. Vol. 10. London: The Palaeontological Association and Wiley-Blackwell; p. 324–355.
Hyder ES, Witton MP, Martil DM. 2014. Evolution of the pterosaur pelvis. Acta Palaeontol Pol. 59:109–124. doi:10.4202/app.2011.1109
Jiang S-L, Li Z-H, Cheng X, Wang X-L. 2020. The first pterosaur basihyal, shedding light on the evolution and function of pterosaur hyoid apparatuses. PeerJ. 8:e8292. doi:10.7717/peerj.8292
Jiang B-Y, Sha J-G. 2006. Late Mesozoic stratigraphy in western Liaoning, China: a review. J Asian Earth Sci. 28(4–6):205–217. doi:10.1016/J.JSEAES.2005.07.006.
Jiang S-X, Zhang X-J, Cheng X, Wang X-L. 2021. A new pteronodontoid pterosaur forelimb from the upper Yixian Formation, with a revision of *Yixianopterus jingangshanensis*. Vertebrata PalAsiatica. 59:81–94. doi:10.19615/J.CNKI.1000-3118.201124
Kaup JJ. 1834. Versuch einer Eintheilung der Säugethiere in 6 Stämme und der Amphibien in 6 Ordnungen. Isis. 1834:311–324.
Kellner AWA. 2003. Pterosaur phylogeny and comments on the evolutionary history of the group. Vol. 217. London: Geol Soc Spec Publ; p. 105–137. doi:10.1144/GSL.SP.2003.217.01.10.
Kellner AWA. 2015. Comments on Triassic pterosaurs with discussion about ontogeny and description of new taxa. An Acad Bras Ciênc. 87(2):669–689. doi:10.1590/0001-3765201520150307.
Kellner AWA, Caldwell MW, Holgado B, Dalla Vecchia FM, Nohra R, Sayão JM, Currie PJ. 2019. First complete pterosaur from the Afro-Arabian continent: insight into pterodactyloid diversity. Sci Rep. 9(1):17875. doi:10.1038/s41598-019-54042-z.
Li J-J, Lü J-C, Zhang B-K. 2003. A new lower cretaceous sinopterid pterosaur from the western Liaoning, China. Acta Palaeontol Sin. 42:442–447.
Lü J-C. 2015. The Hyoid Apparatus of *Liaoxipterus Brachycephalus* [*brachyognathus*] (Pterosauria) and its implications for food-catching behavior. Acta Geol Sin. 36:362–366. doi:10.3975/cagsb.2015.03.13
Lü J-C, Gao Y-B, Xing L-D, Li Z-X, Ji Q. 2007. A New Species of *Huaxiapterus* (Pterosauria: Tapejaridae) from the early cretaceous of Western Liaoning, China. Acta Geol Sin-Engl. 81(5):683–687. doi:10.1111/j.1755-6724.2007.tb00992.x.
Lü J-C, Ji Q. 2005. New Azhdarchid Pterosaur from the early cretaceous of Western Liaoning. Acta Geol Sin-Engl. 79(3):301–307. doi:10.1111/j.1755-6724.2005.tb00893.x.
Lü J-C, Jin X-S, Unwin DM, Zhao L-J, Yoichi A, Ji Q. 2006b. A new species of *Huaxiapterus* (Pterosauria: Pterodactyloidea) from the lower cretaceous of Western Liaoning, China with comments on the systems of Tapejarid Pterosaurs. Acta Geol Sin-Engl. 80:315–326. doi:10.1111/j.1755-6724.2006.tb00251.x
Lü J-C, Liu J-Y, Wang X-R, Gao C-L, Meng Q-J, Ji Q. 2006c. New material of Pterosaur *Sinopterus* (Reptilia: Pterosauria) from the early cretaceous Jiufotang formation, Western Liaoning, China. Acta Geol Sin-Engl. 80:783–789. doi:10.1111/j.1755-6724.2006.tb00302.x
Lü J-C, Teng -F-F, Sun D-Y, Shen C-Z, Li G-Q, Gao X, Liu H-F. 2016. The Toothless Pterosaurs from China. Acta Geol Sin. 90:2513–2525.
Lü J-C, Unwin D-M, Jin X-S, Liu Y-Q, Ji Q. 2010. Evidence for modular evolution in a long-tailed pterosaur with a pterodactyloid skull. Proc R Soc B. 277(1680):383–389. doi:10.1098/rspb.2009.1603.
Lü J-C, Xu L, Ji Q. 2008. Restudy of *Liaoxipterus* (Istiodactylidae: Pterosauria), with comments on the Chinese istiodactylid pterosaurs. Zitteliana. B28:229–241. doi:10.5282/UBM/EPUB.12018
Lü J-C, Yuan C-X. 2005. New Tapejarid Pterosaur from Western Liaoning, China. Acta Geol Sin-Engl. 79(4):453–458. doi:10.1111/j.1755-6724.2005.tb00911.x.
Lü J-C, Zhang B-K. 2005. New Pterodactyloid Pterosaur from the Yixian Formation of Western Liaoning. Geol Rev. 51:458–462.
Martill D-M. 2014. A functional odontoid in the dentary of the Early Cretaceous pterosaur *Istiodactylus latidens*: implications for feeding. Cretaceous Res. 47:56–65. doi:10.1016/J.CRETRES.2013.11.005
Martill D-M, Sweetman S-C, Witton M-P. 2011. Pterosaurs. In: Batten D-J, Sweetman S-C, editors. English Wealden fossils. Field Guides to Fossils. Vol. 14. London: The Palaeontological Association; p. 370–390.
Meng X 2008. A New Species of *Sinopterus* from Jehol Biota and reconstraction of stratigraphic sequence of the Jiufotang Formation. A Thesis for the Master Degree of Science in the Graduate School of Chinese Academy of Sciences. 49 pp.
Pan Y-H, Sha J-G, Zhou Z-H, Fürsich F-T. 2013. The Jehol Biota: definition and distribution of exceptionally preserved relics of a continental Early Cretaceous ecosystem. Cretaceous Res. 44:30–38. doi:10.1016/J.CRETRES.2013.03.007
Peters D. 2011. A catalog of Pterosaur Pedes for Trackmaker identification. Ichnos. 18(2):114–141. doi:10.1080/10420940.2011.573605.
Plieninger F. 1901. Beiträge zur Kenntnis d Flugsaurier. Paläontographica. 48:65–90.
Ruiz-Omeñaca JI, Canudo JI, Cuenca-Bescós G. 1997. Primeros restos de reptiles voladores (Pterosauria: Pterodactyloidea) en el Barremiense superior (Cretácico inferior) de Vallipón (Castellote, Teruel). Mas de les Matas. 17:225–249.
Sánchez-Hernández B, Benton MJ, Naish D. 2007. Dinosaurs and other fossil vertebrates from the Late Jurassic and early cretaceous of the Galve area, NE Spain. Paleogeogr Palaeoclimat Palaeoecol. 249(1–2):180–215. doi:10.1016/J.PALAEO.2007.01.009.
Schmitz L, Motani R. 2011. Nocturnality in Dinosaurs inferred from scleral ring and orbit morphology. Science. 332(6030):705–708. doi:10.1126/science.1200043.
Seeley HG. 1901. Dragons of the air: an account of extinct flying reptiles. New York: D. Appleton, London, Methuen & Co. 240 pp.
Sha J-G. 2007. Cretaceous stratigraphy of northeast China: non-marine and marine correlation. Cretaceous Res. 28(2):146–170. doi:10.1016/J.CRETRES.2006.12.002.
Smith PE, Evensen NM, York D, Chang -M-M, Jin F, Li J-L, Cumbaa S, Russell D. 1995. Dates and rates in ancient lakes: 40 Ar– 39 Ar evidence for an early cretaceous age for the Jehol Group, northeast China. Canadian Journal of Earth Sciences. 32(9):1426–1431. doi:10.1111/j.1755-6724.2007.tb00992.x.
Sweetman SC, Martill DM. 2010. Pterosaurs of the Wessex Formation (Early Cretaceous, Barremian) of the Isle of Wight, southern England: a review with new data. J Iberian Geol. 36(2):225–242. doi:10.5209/JIGE.33858.
Swisher CC III, Wang Y-Q, Wang X-L, Xu X, Wang Y. 1999. Cretaceous age for the feathered dinosaurs of Liaoning, China. Nature. 400(6739):58–61. doi:10.1038/21872.
Swisher CC III, Wang X-L, Zhou Z-H, Wang Y-Q, Jin F, Zhang J-Y, Xu X, Zhang F-C, Wang Y. 2002. Further support for a cretaceous age for the feathered-dinosaur beds of Liaoning, China: new ^{40}Ar-^{39}Ar dating of the Yixian and Tuchengzi Formations. Chinese Sci Bull. 47:136–139. doi:10.1360/02TB9031
Unwin DM. 2003. On the phylogeny and evolutionary history of pterosaurs. Vol. 217 London: Geol Soc Spec Publ; p. 139–190. doi:10.1144/GSL.SP.2003.217.01.11.
Wang S-S, Hu H-G, Li P-X, Wang Y-Q. 2001b. Further discussion on the geologic age of Sihetun vertebrate assemblage in western Liaoning, China: evidence from Ar-Ar dating. Acta Petrol Sin. 17:663–668.

Wang X-L, Kellner AWA, Zhou Z-H, Campos DDA. 2005. Pterosaur diversity and faunal turnover in Cretaceous terrestrial ecosystem in China. Nature. 437 (7060):875–879. doi:10.1038/nature03982.

Wang L, Li L, Duan Y, Cheng S-L. 2006. A new i[sti]odactylid pterosaur from western Liaoning. Geol Bull China. 25:737–740.

Wang S-S, Wang Y-Q, Hu H-G, Li H-M. 2001a. The existing time of Sihetun vertebrate in western Liaoning,China-Evidence from U-Pb dating of zircon. Chinese Sci Bull. 46(9):779–782. doi:10.1007/BF03187222.

Wang X-L, Zhou Z-H. 2003. A new pterosaur (Pterodactyloidea, Tapejaridae) from the early cretaceous Jiufotang formation of western Liaoning, China and its implications for biostratigraphy. Chinese Sci Bull. 48(1):16–23. doi:10.1007/BF03183326.

Wellnhofer MP. 1991. The illustrated Encyclopedia of Pterosaurs. London: Salamander Books. 192 pp.

Witton MP. 2012. New insights into the skull of *Istiodactylus latidens* (Ornithocheiroidea, Pterodactyloidea). PLos One. 7(3):e33170. doi:10.1371/journal.pone.0033170.

Witton MP. 2013. Pterosaurs. New Jersey: Princeton University Press; p. 291. doi: 10.1515/9781400847655.

Wu Z-J, Gao F-L, Pan Y-Q, Wang X. 2018. Division and comparison of Jiufotang Formation of western Liaoning are and its rare fossil bed. Geoscience. 32:758–765.

Xu Y-Z, Jiang S-X, Wang X-L. 2022. A new istiodactylid pterosaur, *Lingyuanopterus camposi* gen. et sp. nov., from the Jiufotang Formation of western Liaoninng, China. PeerJ. 10:e13819. doi:10.7717/peerj.13819

Xu X, Zhou Z-H, Wang Y, Wang M. 2019. Study on Jehol Biota: recent advances and future prospects. Sci China Earth Sci. 49:1491–1511. doi:10.1007/s11430-019-9509-3

Yu Z-Q, Wang M, Li Y-J, Deng C-L, He H-Y. 2021. New geochronological constraints for the Lower Cretaceous Jiufotang Formation in Jiangchang Basin, NE China, and their implications for the late Jehol Biota. Paleogeogr Palaeoclimat Palaeoecol. 583:110657. doi:10.1016/j.palaeo.2021.110657

Zhang X-J, Jiang S-X, Xing C, Wang X-L. 2019. New Material of *Sinopterus* (Pterosauria, Tapejaridae) from the early cretaceous Jehol Biota of China. An Acad Bras Ciêc. 91(suppl 2):e20180756. doi:10.1590/0001-376520192018756.

Zhong Y-T, Huyskens MH, Yin Q-Z, Wang Y-Q, Ma Q, Xu Y-G. 2021. High-precision geochronological constraints on the duration of 'Dinosaur Pompeii' and the Yixian Formation. Natio Sci Rev. 8(6):nwab063. doi:10.1093/nsr/nwab063.

Zhou X-Y, Pêgas RV, Leal MEC, Bonde N. 2019. *Nurhachius luei*, a new istiodactylid pterosaur (Pterosauria, Pterodactyloidea) from the Early Cretaceous Jiufotang Formation of Chaoyang City, Liaoning Province (China) and comments on the Istiodactylidae. PeerJ. 7:e7688. doi:10.7717/peerj.7688

Zhou C-F, Zhu Z-H, Chen J. 2022. First pterosaur from the early cretaceous Huajiying formation of the Jehol Biota, northern Hebei Province, China: insights on the pedal diversity of Pterodactyloidea. Hist Biol. 1–7. doi:10.1080/08912963.2022.2079085